Available online at www.sciencedirect.com
ScienceDirect
Trans. Nonferrous Met. Soc. China 19(2009) 1065−1070
Transactions of Nonferrous Metals Society of China
www.tnmsc.cn

Corrosion behavior of ultra-fine grained industrial pure Al fabricated by ECAP

SONG Dan(宋 丹), MA Ai-bin(马爱斌), JIANG Jing-hua(江静华),
LIN Pin-hua(林萍华), YANG Dong-hui(杨东辉)

College of Materials Science and Engineering, Hohai University, Nanjing 210098, China

Received 21 October 2008; accepted 14 January 2009

Abstract: Corrosion behavior of ultra-fine grained(UFG) industrial Al fabricated by equal channel angular pressing(ECAP) for 16 pass times was investigated by potentiodynamic polarization test, potentiostatic polarization test, electrochemical impedance spectroscopy(EIS) measurement, immersion test and surface analyses (OM and SEM). The microstructures including grain size, grain boundaries and dislocations were also observed by TEM. The results show that the UFG industrial pure Al has more positive pitting potential, less corrosion current density and five times larger passive film resistance compared with the coarse grained(CG) one. It was found that the increased pitting resistance is profited from the more stable passive film kept in the Cl^- aggressive solution due to more grain boundaries, larger fraction of non-equilibrium grain boundaries and residual stress of the UFG industrial pure Al.
Key words: equal channel angular pressing; ultra-fine grain; corrosion behavior; industrial pure Al

1 Introduction

Equal channel angular pressing(ECAP) as one of the most effective methods for fabricating bulk ultra-fine grained(UFG) materials with grain sizes in the range of 10−1000 nm has attracted great attention in the last decade [1]. ECAP has a number of advantages compared with traditional metal process technologies[2−3]. Most investigations on UFG materials fabricated by ECAP were focused on the structural characterization[4−5], thermal stability[6−7], and mechanical properties[8−10], while there were limited works on the corrosion behavior of ECAP processed(ECAPed) materials.

Pure Al and Al alloy have relative good pitting corrosion resistance due to the dense oxide film formed on the surface. Lots of previous works expatiated the pitting corrosion mechanism of Al in normal state like adsorption and penetration of chloride ion on the passive film, pitting initiation and propagation etc[11−12]. But little articles concerned about the corrosion behavior of pure Al in ECAPed state with deformed structure. In this study, the pitting corrosion behavior of the UFG industrial pure Al in the chloride-containing solution was investigated by electrochemical methods, immersion test, surface analysis and microstructure observation techniques. Especially, the effects of deformed microstructure on the passive film and corrosion behavior of the industrial pure Al were studied.

2 Experimental

2.1 ECAPed specimen preparation

The industrial pure Al having the chemical composition of Al-0.5%Si-0.15%Fe was die cast and machined into billets with the size of 20 mm×20 mm×40 mm. The billets were pressed as the illustration shown in Fig.1 for 16 passes with the plunger speed of 0.5 mm/s at room temperature. The graphite was used as lubricant to reduce the friction coefficient between work pieces and die inner wall. According to Ref.[10], more ECAP pass times will benefit the deformed UFG material with higher ultimate tensile strength and ductibility, so extreme 16 pass times were used here to fabricate bulk UFG industrial pure Al without any microcrack.

2.2 Corrosion experiments

The corrosion resistant properties of ECAPed UFG and as-cast coarse grain(CG) industrial pure Al were compared using electrochemical tests. The electro-

Corresponding author: MA Ai-bin; Tel: +86-25-83787239; E-mail: aibin-ma@hhu.edu.cn
DOI: 10.1016/S1003-6326(08)60407-0

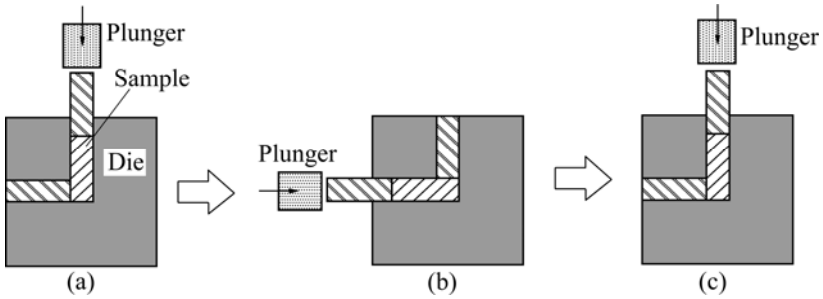

Fig.1 Schematic illustration of ECAP process

chemical experiments were carried out in the 0.01 mol/L sodium sulfate (Na_2SO_4) water solution containing 0.01% Cl^-. In this solution, the Cl^- ion additives induce pit initiation while SO_4^{2-} additives retard the incorporation of Cl^- into the oxide film on industrial pure Al due to the competitive adsorption on the sample surface[13]. Thus, this solution is suitable for observing the pitting resistance and passivation behavior of the cast and ECAPed industrial pure Al. The electrochemical experiments were carried out in the Parstat 2273 advanced potentiostat with the traditional three-electrode system using saturated calomel electrode(SCE) as the reference and Pt electrode as the counter electrode. All electrochemical experiment samples were cut by spark erosion perpendicularly to the pressing direction from the core of ECAPed billets. Then the samples were mounted with epoxy leaving an exposed area of 1 cm^2 on the surface and finally polished for good reproducibility. Each corrosion sample was immersed in the solution for 10 min for achieving the stable open-circuit potential. The potentiodynamic polarization tests were carried out to measure the pitting potential of both samples at the scanning rate of 0.5 mV/s. The potentiostatic polarization tests were carried out to examine the passive film breakdown (pit initiation and propagation) under the pitting potential. The electrochemical impedance spectroscopy(EIS) tests were performed to compare the impedance behaviors between CG and UFG samples.

The corrosion resistances of ECAPed UFG and cast CG industrial pure Al were detected by the immersion test. The square specimens of 10 mm×10 mm×1 mm were cut from the core of sample perpendicularly to the pressing direction and polished for good observation. They were immersed in 3.5% NaCl solution for 3 d at room temperature.

2.3 Microstructure observation and surface analysis

Optical microstructure samples were cut parallelly to the pressing direction, then were electrolytically etched in 2.5% fluoboric acid (HBF_4) at room temperature. Transmission electron microscopy(TEM, JEM2000EX, Japan) was conducted to observe the grain size, grain boundary and dislocation of the UFG industrial pure Al. The thin foils for TEM were parallel to the pressing direction and prepared by twin jet electro-polisher using 10% $HClO_4$+90% alcohol solution at temperature of 7.8 ℃ and electro-polish voltage of 20 V. After potentiostatic polarization measurement, surface morphologies of the samples were immediately examined by scanning electron microscope(SEM, JEM-6360LV, Japan).

3 Results and discussion

The optical micrographs of the UFG sample of industrial pure Al after 16 ECAP passes and the CG samples are shown in Fig.2. After deformation by ECAP, the UFG sample has much finer grain size (Fig.2(a)) than the CG sample which has grain size more than 200 μm (Fig.2(b)), and it is rather difficult to distinguish the grain boundaries except the plastic flow, which can be observed under optical microscope after 16 passes of ECAP.

The potentiodynamic polarization curves of the UFG and CG industrial pure Al in 0.01 mol/L Na_2SO_4 solution containing 0.01% Cl^- are shown in Fig.3(a). Both samples are passivated in the solution and the main corrosion behavior is pitting corrosion. The pitting potential(φ_{pit}) of samples which denotes the pitting resistance is greatly increased from −250 mV (vs SCE) for CG Al to 35 mV for UFG Al. Meanwhile, the corrosion potential of UFG industrial pure Al is −980 mV, lower than that of the CG counterpart (−710 mV). Fig.3(b) shows the potentiostatic polarization curve measured at the constant potential of 35 mV (the pitting potential of the UFG sample) for 1 h. The relation curves between corrosion current density and time are related with the pitting initiation and propagation induced by breakdown of the passive film. The corrosion current density of the UFG sample is only 10% of the CG counterpart, which clearly indicates that the pitting

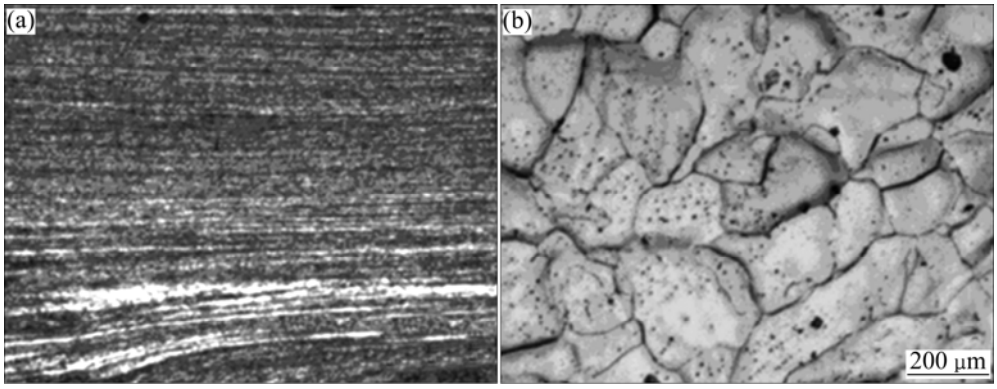

Fig.2 Optical micrographs of industrial pure Al: (a) UFG sample; (b) CG sample

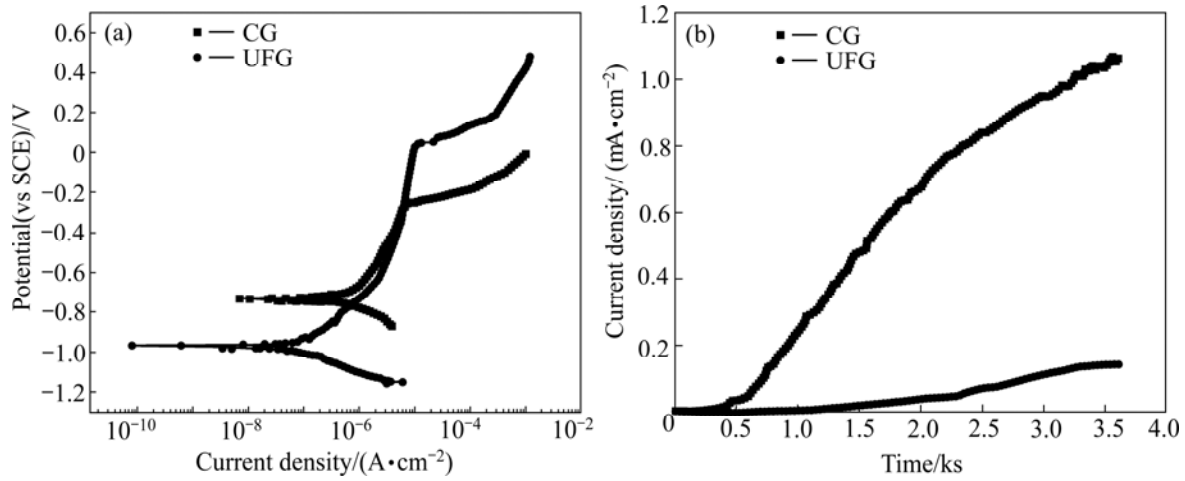

Fig.3 Poloraziation curves of ECAPed UFG and cast CG industrial pure Al in 0.01 mol/L Na_2SO_4 +0.01% Cl^- solution: (a) Potentio-dynamic polarization curve; (b) Potentiostatic polarization curve at pitting potential

resistance has been greatly increased.

Fig.4(a) shows the Nyquist plot of impedance spectra for UFG and CG industrial pure Al at the open circuit potential in 0.01 mol/L Na_2SO_4 solution containing 0.01% Cl^-. The applied frequencies range from 2 MHz to 10 mHz. It shows that both samples have two capacitive loops, one is at high frequencies and the other is at low frequencies. The high frequency loop (the insert in Fig.4(a)) is related to the passivity of Cl^- ion-incorporated layer formed on the surface of the oxide film during the induction period for pit initiation[14]. The size of the first loop is corresponding to the resistance of Cl^- ion-incorporated film. From Fig.4(a), the size of the first loop of the UFG sample is smaller than that of CG one, which indicates that the UFG industrial pure Al has higher resistance to prevent Cl^- from penetrating into the oxide film than CG counterpart. The second capacitive loop appears distorted at low frequencies, which is corresponding to the anodic dissolution of the underlying metal by high field ionic migration through the fresh inner oxide film[15]. In order to determine the resistance of the two-layered oxide film formed in the Cl^--containing solution on UFG and CG industrial pure Al, the measured impedance data were analyzed by ZSimpWin impedance analyzer based on the electric equivalent circuits, which is shown in Fig.4(b) [14]. The corrosion resistance was determined by the resistance of the inner fresh oxide film. According to Fig.4(a), the $R_{inn,\,ox}$ of the UFG sample is 151.95 kΩ, five times that of the CG one (30.25 kΩ), which indicates that the UFG industrial pure Al has higher corrosion resistance than the CG counterpart.

Fig.5 shows the SEM images of the pitting surface morphologies of UFG and CG industrial pure Al after potentiostatic test. The sizes of pits of UFG sample are obviously smaller and distribute more uniformly than those of CG sample. Fig.6 shows the SEM images of the passive film morphology after 3 d immersion in 3.5% NaCl solution. Under the consecutive attack by chloride ion, the passive film of UFG pure Al still kept dense and integral while the CG counterpart had already damaged into some rarefactions (punctuate and crack-like black

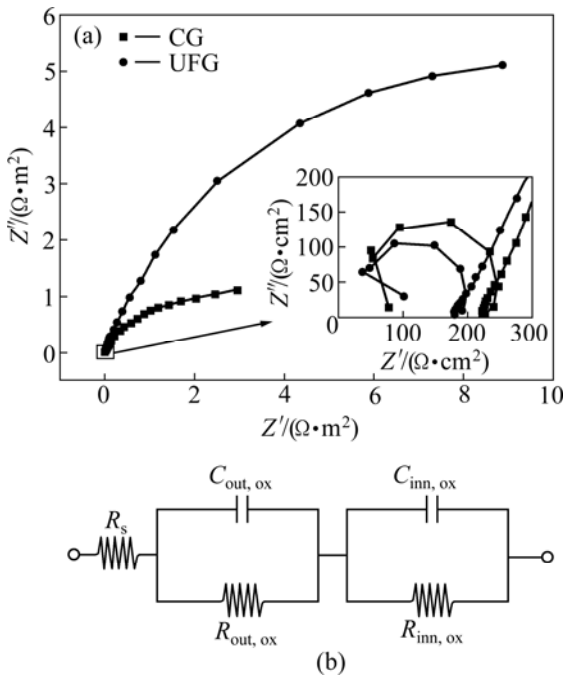

Fig.4 Nyquist plot of impedance spectra of CG and UFG industrial pure Al at passive state (a), and equivalent circuit for native oxide film-covered Al in solution (b) (R_s is solution resistance; $C_{out,\ ox}$ is capacitance of Cl^- ion-incorporated outer film; $R_{out,\ ox}$ is resistance of Cl^- ion-incorporated outer film; $C_{inn,\ ox}$ is capacitance of fresh inner oxide film and $R_{inn,\ ox}$ is resistance of fresh inner oxide film)

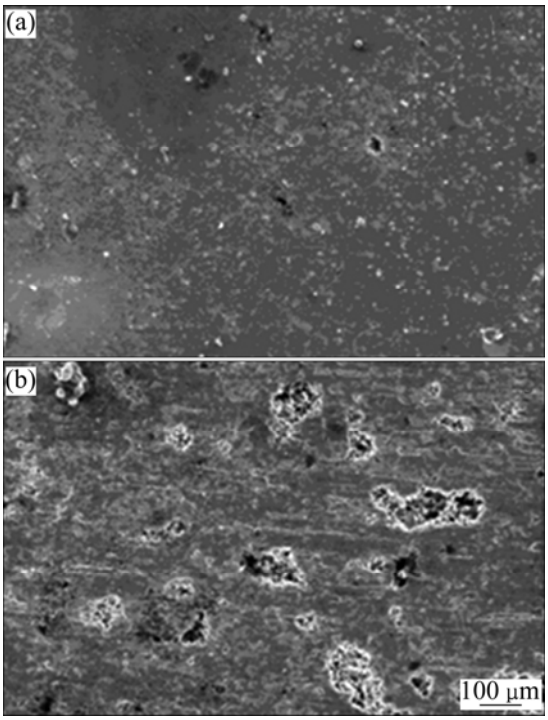

Fig.5 SEM images of pitting surface morphology of industrial pure Al after potentiostatic tests: (a) UFG sample, (b) CG sample

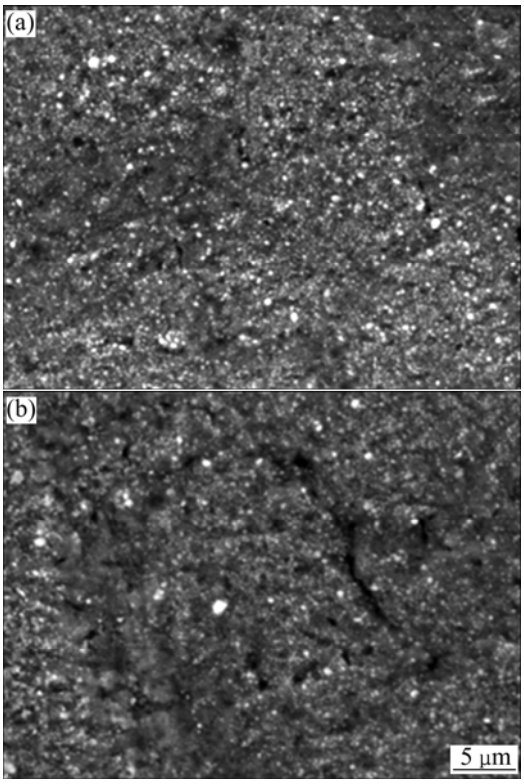

Fig.6 SEM images of passive film morphology after immersion test: (a) UFG sample; (b) CG sample

areas) and exposed Al matrix. This similar phenomenon was also presented in Ref.[16]. From Figs.3−6, one can determine that the UFG industrial pure Al has better pitting resistance than CG one visually.

Fig.7 shows the microstructure and selected area electron diffraction(SAED) pattern of UFG industrial pure Al after 16 ECAP passes. According to the classic equivalent strains equation in Ref.[17], the sample stored nearly more than 16 equivalent strains, which leads to a substantial reduction in grain size, from 200 μm to 0.5 μm in average. Fig.7(b) shows that grains are surrounded by clear and regular shaped boundaries. Dynamic recovery occurs when Al is deformed at room temperature because of the high stack fault energy. The severe strain provides enough energy for dislocation movement: from inside of the grains to the vicinity of the grain boundaries[18]. From Fig.7(b), it can be found that, in the vicinity of boundaries the dislocation density is quite high; while there are nearly free dislocations inside some grains caused by the high dislocation recovery, in some other grains, a number of dislocations are still stored. The quite high dislocation level mentioned above indicates the higher residual stress. The SAED pattern presents a diffused ring with extra spots, indicating large misorientations, referred to non-equilibrium grain boundary caused by great numbers of dislocation accumulated into the grain boundaries[19].

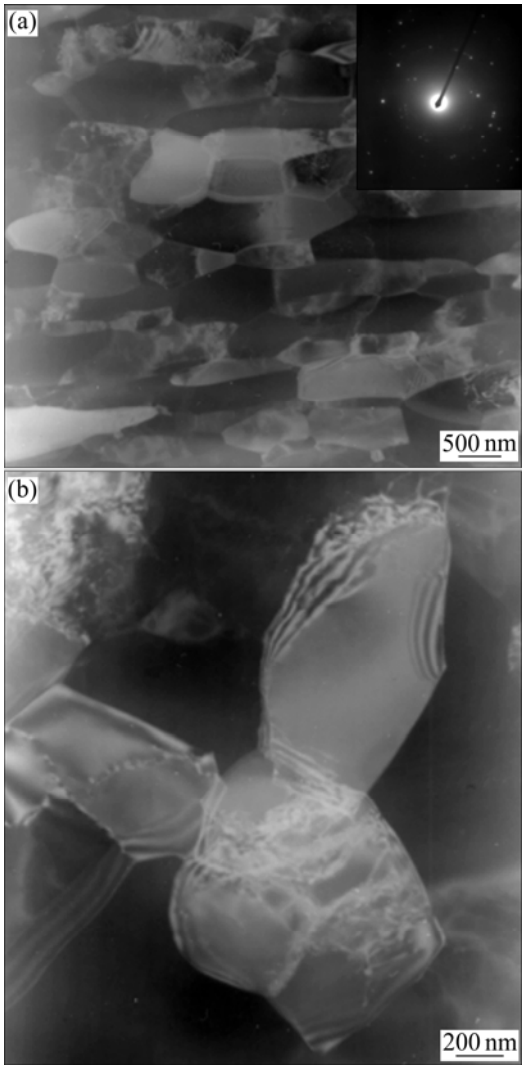

Fig.7 TEM images and SAED pattern of UFG industrial pure Al after 16 ECAP passes

It has been recognized that the grain boundaries play a primary role in many properties of UFG materials. Corrosion in polycrystalline aggregates is also largely associated with interfaces, and moreover, it is sensitive to the grain boundary structure. Corrosion resistance of interfaces immersed in the electrolytic solutions is closely related to their internal energies. The higher the internal energy, the greater the corrosion degradation of the interface region[20]. From the TEM micrographs (Fig.6), the UFG industrial pure Al is characterized by ultra-fined grains with a large fraction of non-equilibrium grain boundaries and high internal energy. Meanwhile, near the grain boundaries and inside of some grains, the dislocation density and residual stress are quite high. The more grain boundaries caused by finer grains, the large fraction of non-equilibrium grain boundaries and high residual stress furnish the UFG industrial pure Al more nucleus to form denser nature oxide film than ordinary CG counterpart. This denser oxide film can be kept relative integral in the aggressive solution and make the UFG sample exhibit better pitting resistance than CG counterpart. Some literatures reported that the silicon-containing impurity particles deteriorate the pitting resistance of the industrial pure Al[21−22]. Meanwhile, ECAP can decrease the size of second phase and particles while refining the grain size[23]. Whether the size of silicon-containing impurity particles will be decreased during ECAP pass times and affect the corrosion performance of UFG industrial pure Al, it needs further studies.

4 Conclusions

1) Ultra-fine grained industrial pure Al with grain size of 0.5 μm can be fabricated by ECAP at room temperature after extreme 16 passes without any microcrack.

2) ECAP has obviously improved the pitting resistance of industrial pure Al. The pitting potential of the UFG industrial pure Al is 35 mV, which is much higher than that of CG one (−250 mV). The corrosion current density of the potentiostatic polarization test of the UFG is 90% less than that of CG one. The resistance of the passive film of the UFG sample is 151.95 kΩ, which is five times that of the CG one.

3) The size and numbers of the pits after potentiostatic polarization for 1 h are decreased in UFG industrial pure Al in comparison with its CG counterpart. After immersion in the 3.5% NaCl solution for 3 d the passive film of UFG industrial pure Al also keeps denser and more integral than the CG one.

4) Increased pitting resistance of UFG Al is attributed to relative dense nature oxide film on the surface. And it is this oxide film，which is caused by more grain boundaries, larger fraction of non-equilibrium grain boundaries and residual stress, that can be kept relative stable and integral in the Cl^--containing solution compared with CG one.

References

[1] VALIEV R A, ALEXANDROV I V. Nanostructured materials obtained by severe plastic deformation [M]. Logos, Moscow, Russia, 2000: 272. (in Russian)

[2] SHIN D H, KIM B C, PARK K T, CHOO W Y. Microstructural changes in equal channel angular pressed low carbon steel by static annealing [J]. Acta Mater, 2000, 48: 3245−3252.

[3] MUKAI T, KAWAZOE M, HIGASHI K. Dynamic mechanical properties of a near-nano aluminum alloy processed by equal-channel-angular-extrusion [J]. Nnostruct Mater, 1998, 10: 755−765.

[4] MURAYAMA M, HORITA Z, HONO K. Microstructure of

two-phase Al-1.7at% Cu alloy deformed by equal-channel angular pressing [J]. Acta Mater, 2001, 49: 21−29.

[5] FERRASSE S, SEGAL V M, KALIDINDI S R, ALFORD F. Texture evolution during equal channel angular extrusion (Part I): Effect of route, number of passes and initial texture [J]. Mater Sci Eng A, 2004, 368: 28−40.

[6] MOLODOVA X, GOTTSTEIN G, WINNING M, HELLMIG R J. Thermal stability of ECAP processed pure copper [J]. Mater Sci Eng A, 2007, 460: 204−213.

[7] EDDAHBI M, del VALLE J A, PEREZ-PRADO M T, RUANO O A. Ultrafine grained steels processed by equalchannel angular pressing [J]. Mater Sci Eng A, 2005, 410: 299−302.

[8] HORITA Z, FUKAWA M, NEMOTO M, BARNES A J, LANGDON T G. Superplastic forming at high strain rates after severe plastic deformation [J]. Acta Mater, 2000, 48: 3633−3640.

[9] VALIEV R Z, LANGDON T G. Principles of equal-channel angular pressing as a processing tool for grain refinement [J]. Prog Mater Sci, 2006, 51: 881−981.

[10] TROEGER L P, STARKE E A Jr. Particle-stimulated nucleation of recrystallization for grain-size control and superplasticity in an Al-Mg-Si-Cu alloy [J]. Mater Sci Eng A, 2000, 293: 19−29.

[11] McCAFFERTY E. Seequennce of steps in the pitting of aluminum by chloride ions [J]. Corrosion Science, 2003, 45: 1421−1438.

[12] LEE W J, PYUN S I. Effects of sulphate ion additives on the pitting corrosion of pure aluminium in 0.01 M NaCl solution [J]. Electrochim Acta, 2000, 45: 1901−1910.

[13] NISANCIOGLU K, HOLTAN H. Cathodic polarization of commercially pure aluminium [J]. Corrosion Science, 1979, 19: 537−552.

[14] LEE W J, PYUM S I. Effects of hydroxide ion addition on anodic dissolution of pure aluminium in chloride ion-containing solution [J]. Electrochim Acta, 1999, 44: 4041−4049.

[15] FOLEY R T, NGUYEN T H. The chemical nature of aluminum corrosion [J]. Electrochem Soc, 1982, 129: 464−467.

[16] WEI Wei, KUN Xia-wei, QING Bo-du. Corrosion and tensile behaviors of ultra-fine grained Al-Mn alloy produced by accumulative roll bonding [J]. Mater Sci Eng A, 2007, 454/455: 536−541.

[17] ZHU Y T, LANGDON T G. Performance and applications of nanostructured materials produced by severe plastic deformation [J]. Scripta Mater, 2004, 51: 825−830.

[18] CHEN Y B, LI Y L, HE L Z, LU C, DING H, LI Q Y. The influence of cryoECAP on microstructure and property of commercial pure aluminum [J]. Mater Letter, 2008, 62: 2821−2824.

[19] VALIEV R Z, ISAMGALIEV R K, ALEXANDROV I V. Bulk nanostructured materials from severe plastic deformation [J]. Prog Mater Sci, 2000, 45: 103−189.

[20] AUST K T, ERB U, PALUMBO G. Interface control for resistance to intergranular cracking [J]. Mater Sci Eng A, 1994, 176: 329−334.

[21] Metals handbook, Vol.13, Corrosion [M]. 9th ed. ASM International: 1987: 583−609.

[22] SERI O, FURUMATA K. Effect of Al-Fe-Si intermetallic compound phases on initiation and propagation of pitting attacks for aluminum 1100 [J]. Mater Corros, 2002, 53: 111−120.

[23] XU C, FURUKAWA M, HORITA Z, LANGDON T G. Influence of ECAP on precipitate distributions in a spray-cast aluminum alloy [J]. Acta Mater, 2005, 53: 749−758.

(Edited by YUAN Sai-qian)